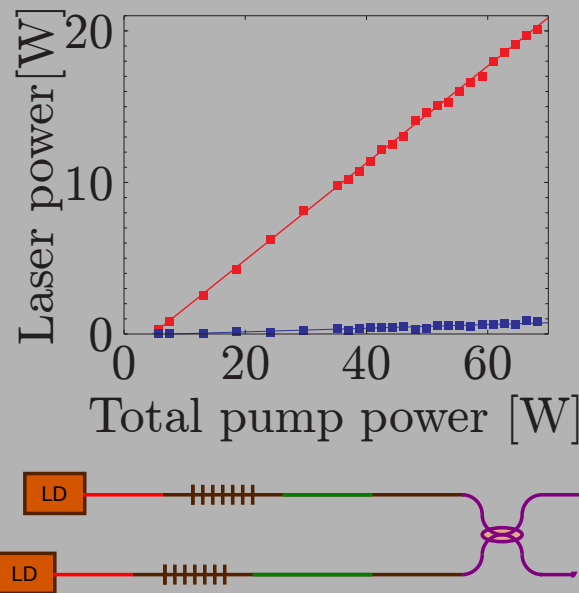


**Abstract:** We experimentally demonstrated coherent beam combining of a pair of thulium-doped fiber lasers using an all-fiber Fox-Smith resonator. We built two thulium-doped fiber lasers from PM fibers and pumped them at 793 nm. Each laser provided a power of more than 10 W at a wavelength of 2000 nm with a slope efficiency of more than 0.5. Then a compound Fox-Smith resonator was created using the PM coupler. Obtained laser power was more than 20 W due to a constructive interference at the output of the laser while a slope efficiency decreased to a value of 0.35. A stable CW output signal was achieved despite the fact that the individually operated lasers had tendency to self-pulsate.

The coherently combined thulium doped fiber laser and its output power as a function of the total launched pump power.



Copyright line will be provided by the publisher

## Coherently combined power of 20 W at 2000 nm from a pair of thulium-doped fiber lasers

*P. Honzatko,<sup>1,\*</sup> Y. Baravets,<sup>1</sup> F. Todorov,<sup>1</sup> P. Peterka,<sup>1</sup> and M. Becker<sup>2</sup>*

<sup>1</sup> Institute of Photonics and Electronics, Academy of Sciences of the Czech Republic, v.v.i., Chaberska 57, 182 51 Prague, Czech Republic

<sup>2</sup> Institute of Photonic Technology, Albert Einstein Str. 9, 07745 Jena, Germany

Received: XXXX, Accepted: XXXX

Published online: XXXX

**Key words:** thulium-doped fiber laser; laser beam combining

### 1. Introduction

Material processing, medicine and environment monitoring by lidars demand for powerful laser sources with a flexible selection of wavelengths. Diode-pumped single-mode fiber lasers combine high efficiency of laser diodes with excellent beam quality of fiber lasers. High-power ytterbium-doped fiber lasers working in a spectral range of 1060-1100 nm have practically become a standard tool for fine cutting, welding and engraving

of metals. Other wavelengths are needed for plastics processing, biological tissue cutting, etc., in order to achieve high absorption in the material being processed. Thulium-doped fibers are very perspective for such applications because they allow an efficient pumping and provide extremely wide gain-bandwidth. The power of CW thulium-doped fiber lasers (TDFL) has been pushed to a kW level recently [1].

Optical fibers heavily doped by thulium allow an efficient cross-relaxation process when they are pumped

\* Corresponding author: honzatko@ufe.cz

Copyright line will be provided by the publisher

at a wavelength of 793 nm. The cross-relaxation allows to excite two thulium ions for each absorbed pump photon [2]. A low quantum defect and subsequently a low thermal load can be obtained in this way, making such fibers suitable for high-power lasers. A power of 137 W and a slope efficiency of 0.62 was achieved in an all-fiber TDFL at a wavelength of 2019 nm [3]. Amplification of the signal from a single-frequency diode laser to an output power of 608 W was demonstrated in a four-stage fiber amplifier at a wavelength of 2040 nm [4].

Scaling the power of single mode fiber lasers is limited by optical or thermal damage of the fiber, thermal aberrations, and nonlinear effects [5, 6]. A promising approach to scaling the power of fiber lasers up is beam combining, where several laser beams are merged into a single output beam. There are generally two laser beam combining schemes. One scheme relies on a coherent beam combining, where several mutually coherent beams with identical wavelengths are superposed in such a way that constructive interference occurs at the output of the laser. The second scheme is represented by a spectral beam combining, where the beams with differing wavelengths are spatially overlapped using a diffractive element [7].

Two all-fiber schemes are commonly used for passive coherent combining of fiber lasers. In one of them, active fibers are included in branches of the Mach-Zehnder interferometer [8, 9]. In the other scheme, active fibers are inserted in branches of the Michelson interferometer [10]. The later scheme is usually referred to as a Fox-Smith resonator. A theoretical treatment of this scheme that takes into account transient gain dynamics of the active fibers can be found in [11].

The concept of coherent combining was proved for the erbium [8–10, 12], neodymium [13] and thulium [14] fiber lasers at low powers, and for ytterbium fiber lasers also at moderate powers [15–17]. The power of the coherently combined TDFL was limited to 5 mW in the experiment of Pu Zhou *et al.* [14].

In this paper we demonstrate coherent combining of signals from two thulium-doped fiber lasers. We achieved an output power of 20 W at a wavelength of 2000 nm. A stable CW regime was achieved despite the fact that constituent lasers had a strong tendency to self-pulsations when operated individually. We believe that this is the first demonstration of coherently combined thulium-doped fiber lasers performed at moderate powers.

## 2. Constituent lasers

The topology of the constituent thulium-doped fiber lasers (TDFL) is shown in Fig. 1. A resonator consists of an active fiber, a fiber Bragg grating (FBG) and

a partially reflecting output mirror. We use a polarization maintaining thulium-doped double-clad fiber (PM-TDF-10P/130-HE, Nufern) as an active fiber. The fiber has a core diameter of 10  $\mu\text{m}$  and an inner-cladding diameter of 130  $\mu\text{m}$ . It is covered by a low index polymer coating with a diameter of 215  $\mu\text{m}$ . The numerical apertures of the core and the inner cladding are 0.15 and 0.46, respectively. The stress elements of the Panda-like fiber randomize the ray paths of pump radiation in the inner cladding so that neither the inner cladding shaping nor the special fiber winding is necessary to make the skew rays to cross the core. We built two lasers with 4.5 m, and 3.5 m length of the active fiber, respectively. The ac-

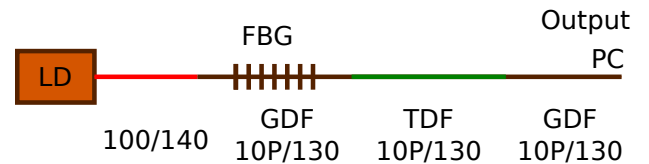


**Figure 1** Scheme of a constituent thulium-doped fiber laser. TDF–thulium-doped fiber, GDF–geometry-matched passive germanium-doped fiber, FBG–fiber Bragg grating, LD–pump laser diode, PC–perpendicularly cleaved fiber end.

tive fiber is spliced to the germanium-doped double-clad fiber (GDF) with matched refractive index profile (GDF-10P/130, Nufern). The highly reflective FBG is written directly into the GDF with two beam interferometry and a deep ultraviolet femtosecond laser source [18]. This inscription method allows to inscribe highly reflective FBG without hydrogen loading. Two

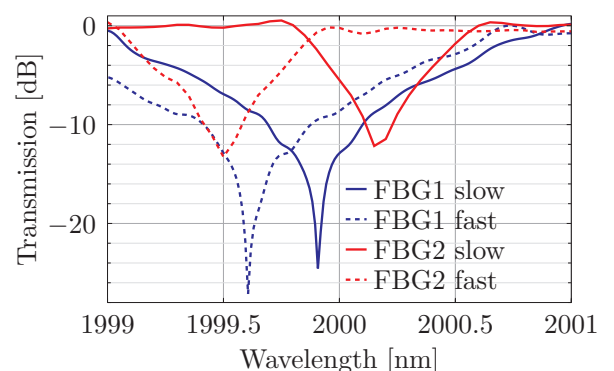


**Figure 2** Transmission function of the FBGs written into GDFs.

FBGs were fabricated for use in TDFLs. Their resonance wavelengths were designed to be 2000 nm.

The transmission functions of the FBGs were measured with a FTIR spectrometer with a resolution of  $0.25 \text{ cm}^{-1}$ . Results are shown in Fig. 2. The resonance is split as a result of birefringence. Slightly different transmission profiles and frequency splittings were observed for these two gratings, probably as a result of different orientation of the fiber during the grating inscription process.

The active fiber is pumped by a multimode laser diode at 793 nm (Limo, LIMO35-F100-DL793-EX1399). The laser gives a power up to 35 W that is coupled into a 100/140  $\mu\text{m}$  multimode fiber with a NA of 0.22 (Limo). The temperature of the diode is kept constant using a pair of Peltier elements with an overall available cooling power of 90 W. The dependence of the mean wavelength and the output power on the laser diode current is shown in Fig. 3. The laser diode has a threshold of 10.9 W and a conversion efficiency slope of 0.92 W/A. The mean wavenumber  $\bar{\nu}$  is defined as

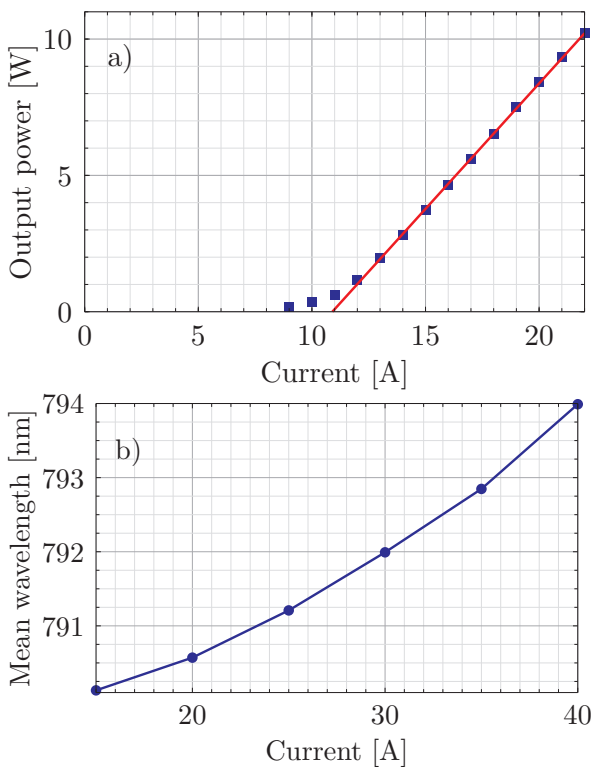


**Figure 3** Dependence of (a) an output power, and (b) a mean wavelength on the pump laser diode current.

$$\bar{\nu} = \frac{\int S(\tilde{\nu})\tilde{\nu}d\tilde{\nu}}{\int S(\tilde{\nu})d\tilde{\nu}}, \quad (1)$$

where  $S(\tilde{\nu})$  is a spectral power density as a function of wavenumber  $\tilde{\nu}$ . The mean wavelength is then  $\bar{\lambda} =$

$10^7/\bar{\nu}$  with a wavelength expressed in nanometers and a wavenumbers measured in  $[\text{cm}^{-1}]$ .

The fiber from the pump laser diode is tapered and spliced to the GDF and the pump power propagates through the FBG toward the active fiber. The opposite side of the active fiber is spliced to a short length of GDF that is perpendicularly cleaved to form an output mirror. The active fiber is coiled on an 11 cm diameter aluminum mandrel to favor the cooling. The splices are recoated with a low index acrylate and are passively cooled.

### 3. Coherently combined laser

The constituent lasers are spliced to a PM coupler (Evanescent Optics) as it is shown in Fig. 4. A large difference in the lengths of the constituent lasers makes a mode structure of the compound cavity sufficiently dense and facilitates mutual injection locking. The PM coupler is fabricated in such a way that properly aligned PM fibers are glued in silica substrate blocks, side polished leaving the core intact and brought into optical contact. The coupler has an excess insertion loss of 7% and it is passively cooled. The idler port is terminated with a FC/APC connector to suppress the reflection while the output port is perpendicularly cleaved and serves as a low reflectivity output mirror. The laser diodes are driven independently so that we can pump either any one of the lasers or both of them.

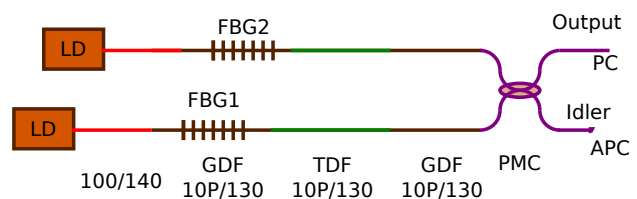


**Figure 4** Scheme of a coherently combined laser. TDF–thulium-doped fiber, GDF–geometry-matched passive germanium-doped fiber, FBG–fiber Bragg grating, LD–pump laser diode, PMC–polarization maintaining coupler, PC–perpendicularly cleaved fiber end, APC–angle polished connector

### 4. Experimental results and discussion

First we investigated the behavior of constituent lasers (Fig. 1). The measured output power as a function of the launched pump power for one of the lasers is shown in Fig. 5. The laser has a threshold of 1.75 W

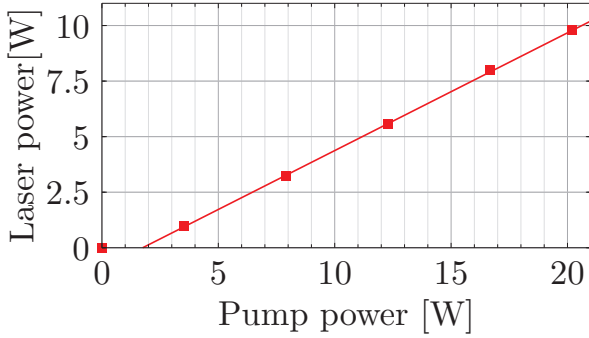


**Figure 5** Pump power dependence of the constituent laser power.

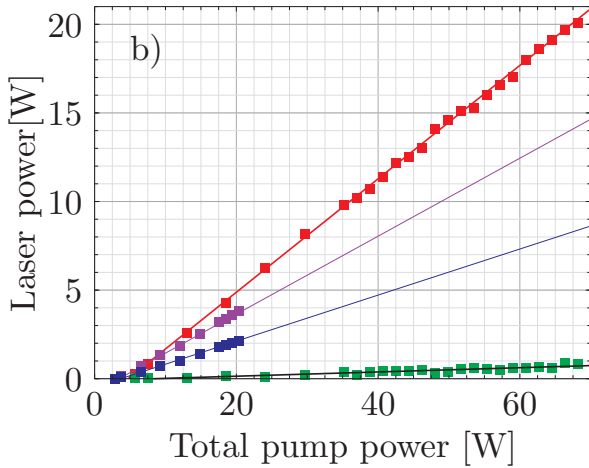


**Figure 6** The laser power for the first (purple), second (blue), and both (red) branches pumped, and the idler (green) for both branches pumped.

and a slope efficiency of 0.53. The slope efficiency compares well to other results for TDFL [3].

Then we studied behavior of coherently combined laser (Fig. 4). The measured laser power as a function of the total launched pump power is shown in Fig. 6. We achieved more than 20 W of output power. The slope efficiency decreased from 53% measured for the constituent lasers to 35%. The coupler used to coherently combine laser signals had a coupling ratio quite distinct from 0.5. We measured a coupling ratio of 0.54/0.39 and 0.59/0.34 for the slow and fast axes, and an excess insertion loss of 0.3 dB. Despite this fact we observed only a small power at the idler output (green points in Fig. 6). Due to a self-adjustment of the phase, the idler is formed by a difference of bar

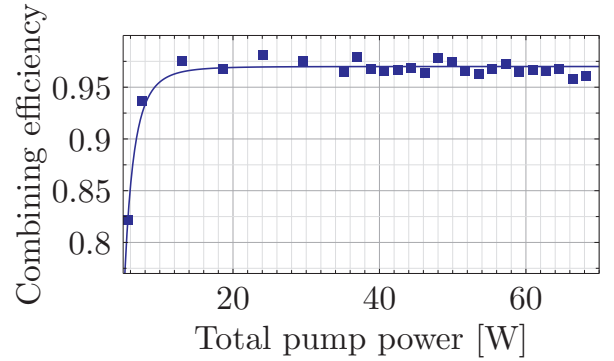


**Figure 7** The combining efficiency as a function of the total launched pump power.

and cross coupled signals

$$P_I = P_L R \left( \sqrt{tG_1 R_{FBG1} r} - \sqrt{rG_2 R_{FBG2} t} \right)^2 / (1-R) \quad (2)$$

where  $P_I$  is the power at the idler output,  $P_L$  is the output power of the laser,  $R$  is the reflection coefficient of the perpendicularly cleaved fiber end (3.5%),  $G_{1,2}$  are gains of the active fibers,  $R_{FBG1,2}$  are reflection coefficients of the FBGs that are close to 1, and  $t, r$  are intensity bar- and cross-coupling coefficients of the coupler. The gain of both active fibers is approximately the same in the regime of saturation and therefore the idler is close to zero even for unequal splitting ratios. The results in Fig. 6 are shown for equal currents of the pump diodes. Even better cancellation of the idler can be achieved if the currents of the pump diodes are properly adjusted. The tolerance of this combining scheme with respect to intensity imbalance has already been mentioned by Sabourdy *et al.* [8].

In Fig. 6 we compare the laser power for the coherently combined signal (red) and for the individually pumped active fibers (purple, blue). It should be noted that the threshold of the individually operated lasers is elevated with respect to independent constituent lasers (Fig. 5) as a result of additional loss inserted by the coupler. Imbalance of the coupler leads to unequal slopes of the lasing characteristics that are 0.13 and 0.22, respectively.

The combining efficiency

$$\eta = \frac{P_L}{P_L + P_I}. \quad (3)$$

is shown in Fig. 7 and it achieves asymptotically a value of 0.97. We did not observe deterioration of combining efficiency at high pump powers in contrast to [17]. We also investigated the dynamics of the coherently combined laser. It is known that thulium-doped fiber lasers have tendency to self-pulsing [19].

We observed chaotic pulsations on a characteristic microsecond time-scale at all pump levels when the constituent lasers were pumped separately (Fig. 8a). The coherently combined signal of the laser was stable in a whole range of pump powers when both constituent lasers were pumped (Fig. 8b). For the measurements we used an InGaAs detector with a relaxation time of 30 ns.

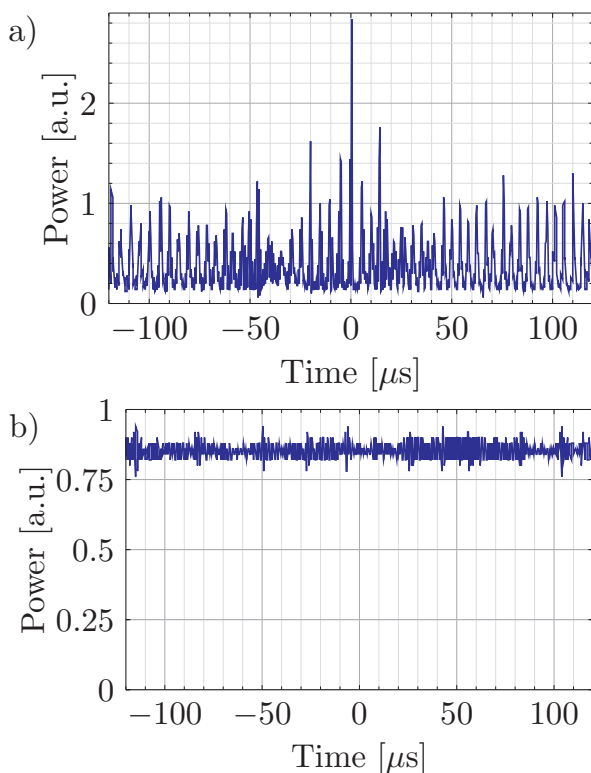


**Figure 8** The output signal when (a) one branch is pumped, (b) both branches are pumped.

## 5. Conclusions

We coherently combined signal from two thulium-doped fiber lasers coupled with a fiber coupler. We demonstrated the robustness of this scheme with respect to unequal splitting ratio of the coupler. We achieved more than 20 W of output power. The slope efficiency decreased from 53% of constituent lasers to 35% for coherently combined laser. The coherently combined signal was stable in the whole range of pump powers despite the fact, that constituent lasers were self-pulsing when operated individually.

*Acknowledgements* We gratefully acknowledge funding of this work by the Czech Science Foundation under Grant No. P205-11-1840.

## References

- [1] T. Ehrenreich, R. Leveille, I. Majid, K. Tankala, G. Rines, and P. Moulton 1-kW, all-glass Tm: fiber laser, SPIE Photonics West 2010: LASE, Fiber Lasers VII: Technology, Systems and Applications, Conference 7850, San Francisco, California, United States, 28. Jan. 2010.
- [2] S.D. Jackson, *Optics Communications* **230**(1-3), 197–203 (2004).
- [3] Y. Tang, C. Huang, S. Wang, H. Li, and J. Xu, *Opt. Express* **20**(16), 17539–17544 (2012).
- [4] G.D. Goodno, L.D. Book, and J.E. Rothenberg, *Optics Letters* **34**(8), 1204–1206 (2009).
- [5] J.W. Dawson, M.J. Messlerly, R.J. Beach, M.Y. Shverdin, E.A. Stappaerts, A.K. Sridharan, P.H. Pax, J.E. Heebner, C.W. Siders, and C. Barty, *Opt. Express* **16**(17), 13240–13266 (2008).
- [6] D.J. Richardson, J. Nilsson, and W.A. Clarkson, *Journal of the Optical Society of America B* **27**(11), B63–B92 (2010).
- [7] S.J. Augst, A.K. Goyal, R.L. Aggarwal, T.Y. Fan, and A. Sanchez, *Optics Letters* **28**(5), 331–333 (2003).
- [8] D. Sabourdy, V. Kermene, A. Desfarges-Berthelemot, L. Lefort, A. Barthelemy, P. Even, and D. Pureur, *Opt. Express* **11**(2), 87–97 (2003).
- [9] S.P. Chen, Y.G. Li, and K.C. Lu, *Optics Express* **13**(20), 7878–7883 (2005).
- [10] A. Shirakawa, T. Saitou, T. Sekiguchi, and K. Ueda, *Optics Express* **10**(21), 1167–1172 (2002).
- [11] T.W. Wu, W.Z. Chang, A. Galvanauskas, and H.G. Winful, *Opt. Express* **18**(25), 25873–25886 (2010).
- [12] T. Simpson, A. Gavrielides, and P. Peterson, *Opt. Express* **10**(20), 1060–1073 (2002).
- [13] H. Bruesselbach, D.C. Jones, M.S. Mangir, M. Minden, and J.L. Rogers, *Optics Letters* **30**(11), 1339–1341 (2005).
- [14] P. Zhou, X. Wang, Y. Ma, H. Ma, K. Han, X. Xu, and Z. Liu, Active and passive coherent beam combining of thulium-doped fiber lasers, in: Proc. SPIE, edited by U.N. Singh, D. Fan, J. Yao, and R.F. Walter, High-Power Lasers and Applications V Vol. 7843 (2010).
- [15] H. Bruesselbach, M. Minden, J.L. Rogers, D.C. Jones, and M.S. Mangir, 200 W self-organized coherent fiber arrays, in: Technical Digest (CD), (Optical Society of America, May 2005), pp. CMDD4.
- [16] B. Wang, E. Mies, M. Minden, and A. Sanchez, *Opt. Lett.* **34**(7), 863–865 (2009).
- [17] B. Wang and A. Sanchez, *Optical Engineering* **50**(11), 111606–111606 (2011).
- [18] M. Becker, J. Bergmann, S. Bruckner, M. Franke, E. Lindner, M.W. Rothhardt, and H. Bartelt, *Opt. Express* **16**(23), 19169–19178 (2008).
- [19] Y.L. Tang and J.Q. Xu, *Ieee Journal of Quantum Electronics* **47**(2), 165–171 (2011).